OLED5-1
Invited

Operando Sum-Frequency Generation Spectroscopy of High-Efficiency OLEDs for Probing the Charge Carrier Activity

Takayuki Miyamae

t-miyamae@chiba-u.jp
Graduate School of Engineering, Chiba University, 1-33 Yayoi-cho, Inage-ku, Chiba 263-8522, Japan

Keywords: OLEDs, Operando measurement, sum frequency generation, High-efficiency Blue-OLED.

ABSTRACT

Buried organic layers in OLEDs during operation have been investigated using electric-field-induced doubly-resonant sum-frequency generation (EFI-DR-SFG). DC electric field leads to a significant increase in the SFG intensity produced by the charged carriers. We also report the time-resolved EFI-SFG technique, which allows us to observe the carrier transportation non-destructively.

1 INTRODUCTION

Currently, organic light-emitting diodes (OLEDs) have attracted significant attention as next-generation display devices and are beginning to be used in mobile phones and OLED television sets [1,2]. OLEDs also exhibit potential for providing energy savings in a range of applications, including lighting and flexible panel displays. The emission efficiency and device reliability of OLEDs have improved since Tang and Vanslyke reported high-efficiency double-layer OLEDs in 1987 [3]. In their structure, OLEDs have a characteristic multilayered structure, where each organic layer has a different function. Especially, the interfacial structures and properties of the OLEDs are extremely important in determining their charge carrier activity, since both the charge transport and the charge densities in organic layers are directly associated with the performance of the OLEDs. Therefore, examination of the carrier activity in OLEDs under operation is required for analysis of the high-performance OLEDs. Recently, we have developed in probing the charge accumulation state in the buried organic layers in OLEDs during operation by electric-field-induced doubly-resonant sum-frequency generation (EFI-DR-SFG) spectroscopy [4,5]. When a DC electric field $\mathbf{E}_0$ is applied to the device, it leads to a significant increase/decrease in the SFG intensity produced by the internal charged carries. Furthermore, we have reported the direct observation of the real-time carrier behavior in OLEDs by time-resolved EFI-DR-SFG technique [6]. The use of these new techniques allows us to observe the carrier behavior at the buried organic interfaces of OLEDs varied with time in response to the applied bias voltage non-destructively.

In this paper, we herein report the direct observation of the intrinsic degradation behavior by long-term operation of the OLEDs, charge injection, transport, and accumulation behavior in OLED devices by EFI-DR-SFG and time-resolved EFI-DR-SFG.

2 EXPERIMENT

The DR-SFG system employed in this experiment was described in detail in an earlier publication [7]. To avoid laser irradiation damage to the samples, the fluence of the visible beam was kept below 5 μJ per pulse. The absence of damage was confirmed by repeated SFG measurements. The incident angles of the visible and infrared beams were 70 ° and 50 ° from the surface normal, respectively. The signal was averaged over 200 pulses by a gated integrator for every data point taken in a 3 cm^{-1} interval. Depletion of the IR beam by water vapor was minimized by purging the optical path of the IR beam and the sample stage with dry nitrogen gas. All the reported SFG spectra were taken with a PPP polarization combination in which the IR, visible, and SFG light were polarized in the plane of incidence.

For the time-resolved experiments, multilayer OLEDs were operated with the application of a square wave pulse voltage using a pulse delay generator and a high-speed bipolar amplifier [6]. Transient EL emission from the OLEDs was monitored using a photomultiplier and was stored by an oscilloscope.

3 RESULTS AND DISCUSSION

3.1 Operando SFG of pristine and aged OLEDs [5]

Figure 1 shows the EFI-DR-SFG spectra of the fluorescent OLED device (IZO (150 nm)/HAT-CN (25 nm)/α-NPD (45 nm)/Alq_3 (60 nm)/LiF (1.5 nm)/Al (150 nm) on a CaF_2 substrate) at various biasing voltages. All the spectra were taken at the visible wavelength of 460 nm. The SFG curve of the OLED device with no applied voltage shows peaks originate from Alq_3. When we applied a forward bias, the intensities of these Alq_3 SFG peaks are immediately reduced, but those of the peaks at 1584 and 1610 cm^{-1}, in which these peaks are derived from α-NPD, are increased with increasing forward bias voltage [4]. The intensities of the SFG of the α-NPD peaks showed significant voltage dependence due to the internal electric field generated by accumulated carriers in the α-NPD layer, and this behavior can be explained in terms of an electric field induced effect.

With respect to the thicknesses of the organic layers

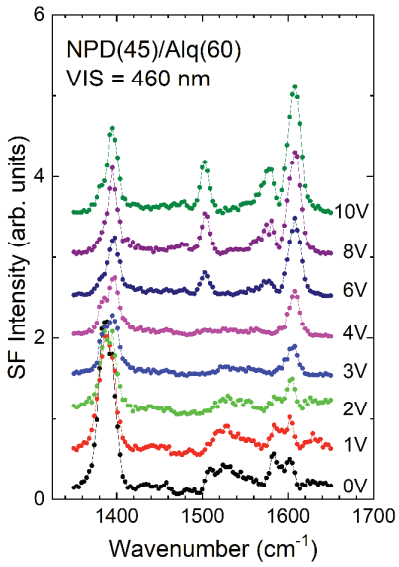

Fig. 1 EFI-DR-SFG spectra of fluorescent double-layer OLED device under various applied voltages at a visible excitation wavelength of 460 nm [5].

consist of the Alq_3 based fluorescent OLED devices, the SFG spectral intensities are larger for the devices with a thicker Alq_3 layer, and they are almost independent of the α-NPD layer thickness. This result indicates that the intensities of the SFG signal strengths of Alq_3 are correlated with the thickness of the Alq_3 layer. It is well documented that Alq_3 molecules show spontaneous non-centrosymmetric orientational ordering of their permanent dipole due to vacuum deposition [8]. This observation clearly indicates that the SFG analyses can detect the molecular ordering information inside OLEDs.

Figure 2 shows the SFG spectra of the pristine and aged OLEDs without applying the bias voltage. While the peak positions and the widths of the SFG spectra of the aged OLED are the same as those of the pristine OLED, remarkable reductions in all the SFG intensities derived from Alq_3 were observed in the aged OLEDs as compared with those of the pristine OLEDs. From the fitting of the spectra, the SFG peak strengths derived for the Alq_3 in the aged OLEDs (LT 50) are about 50 % decreased as compared with the pristine device [5]. We attribute this

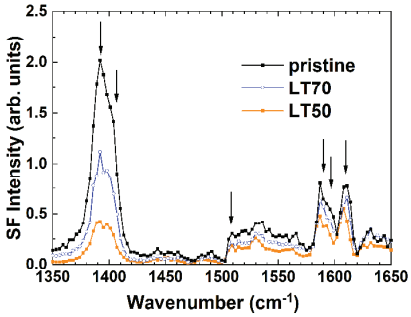

Fig. 2 SFG spectra of pristine and aged OLEDs without applying bias voltage [5]. Arrows indicate the peaks derived from Alq_3.

SFG signal decay is due to the randomization of the permanent dipole ordering of Alq_3 layer. The applied voltage dependence of the SFG peak intensities of Alq_3 support this conclusion. Interestingly, the decrease in the Alq_3 peak strengths depends on the decay of the luminance [5]. We note that such rearrangement of the permanent dipole orientation of Alq_3 layer is not observed in the case of the electron transport Alq_3 layer in the phosphorescent OLED. The difference of Alq_3 layer behavior between aged fluorescent and phosphorescent OLEDs must be caused by the difference of the role of the Alq_3 layer in these devices. It should be noted that the recombination and formation of excited states on Alq_3 molecules occur in the fluorescent devices.

3.2 Operando SFG analysis of high-efficiency blue OLED [9]

Compared to red and green phosphorescent OLEDs, the efficiency and lifetime of blue fluorescent OLEDs are much lower because enough phosphorescent materials have not been developed yet. One way to improve the efficiencies and lifetimes of blue fluorescent OLEDs is to use up-conversion based on the triplet–triplet annihilation (TTA) process, which has been employed to boost the fluorescent light emission [10]. Figure 3 shows the structure of a multilayer blue-OLED device, the I–V characteristics, emission spectrum, and the luminance decay of the blue OLEDs used in this study. External quantum efficiency (EQE) of this OLEDs is around 10%, and the luminance decayed by ca. 5% after 1000 h of continuous driving at an initial luminance of 1000 cd/m^2. Such high EQE is given by the additional TTA process.

In Fig. 4, we show the EFI-DR-SFG spectra of this blue-OLEDs at various DC biasing voltages. When we applied a forward bias, the SFG spectra changes drastically, due to the electric-field induced effect caused

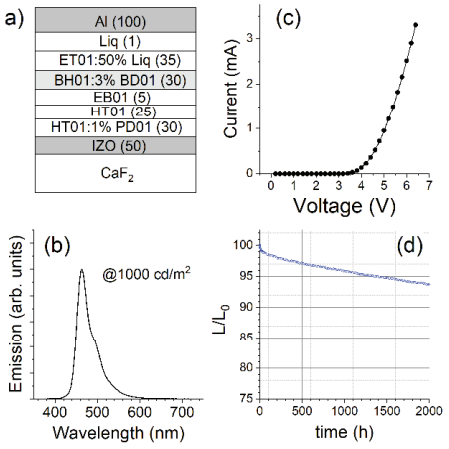

Fig. 3 (a) Device structure of the blue-OLED. (b) Emission spectrum and (c) I–V characteristics of the blue-OLED device. (d) Normalized luminance vs. operating time.

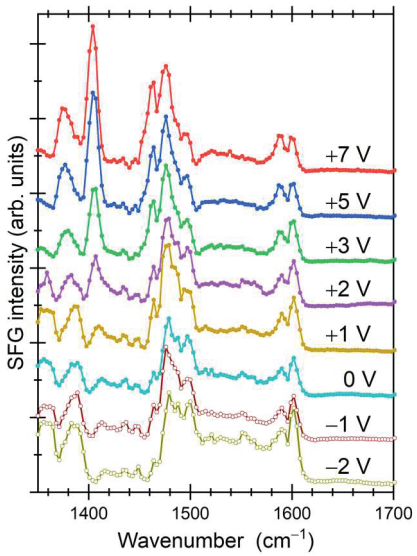

Fig. 4 (a) EFI-SFG spectra of blue-OLED under applied bias voltages from −2 to +7 V [9].

by the internal electric field generated by the injected charged carriers [4].

To determine the origin of the peaks in the EFI-DR-SFG spectra of blue-OLED under operating conditions, we also performed SFG measurements for hole-only devices (HODs) comprising IZO/MoO_3/X/MoO_3/Al, where X indicates HT01:PD01 (1%), HT01, EB01, BH01:BD01 (3%), ETM01:Liq (50%), and Liq. The SFG spectra of each layer of the HODs are shown in Fig. 5. By comparing the SFG spectra of blue OLED with those from each HOD, based on the consistency between the wavelengths of the optical transitions and the SFG output, the peaks observed at 1404 and 1464 cm^{-1}, which increase in intensities by applying a forward bias, are derived from the emission and electron blocking layers, respectively. We attribute the

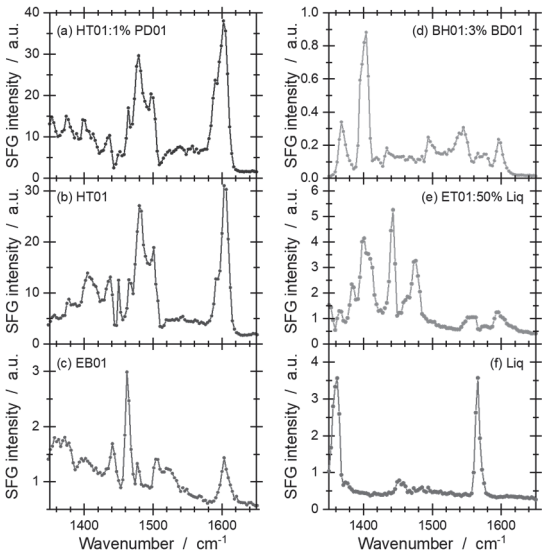

Fig. 5 SFG spectra for hole-only devices without bias voltage [9]. (a) HT01 doped with 1% PD01. (b) HT01. (c) EB01. (d) BH01 doped with 3% BD01. (e) ETM01 doped with 50% Liq. (f) Liq.

SFG peak at 1601 cm^{-1} to the hole-transport material, HT01. Increase in the SFG peak intensities of the peaks derived from the emission layer and the electron blocking layer clearly indicates that the injected charges are accumulated at the interface between emission layer and the electron blocking layer. This conclusion is consistent with the experimental result that the emission occurs at the electron blocking layer / emission layer interface. These observations enable us to understand the real-time charge carrier behavior in various multilayer OLEDs using non-destructive methods.

3.3 Time-resolved SFG of high-efficiency blue OLED

Next, we introduce the direct observation of the charge injection, transport, and accumulation behavior in blue-OLED devices by time-resolved EFI-SFG technique. The use of this technique allows us to investigate that charge carrier generation and recombination at the organic interfaces varied with time in response to the applied pulse bias voltage. These observations therefore enable us to understand the real-time charge carrier behavior inside of the various multilayer OLEDs non-destructively.

The transient EL emission of the blue-OLED device under application of the square-wave pulse bias are shown in Fig. 6. EL emission begins after 1 μs following a charge injection. Furthermore, the delayed fluorescence caused by the TTA process can be clearly observed in the transient EL emission. On the other hand, SFG peak intensities at 1404 (BH01) and 1467 (EB01) are increased just after the pulse injection, and these changes in intensities are almost finished before starting the EL emission.

To observe the charge injection behavior in more detail, Figure 7 shows a magnified scale of the rising edge around the charge injection. The intensity of the SFG signal comes from the host material of the emission layer (black dots, 1404 cm^{-1}, BH01) increase very quickly after the bias application. Interestingly, the rising edge

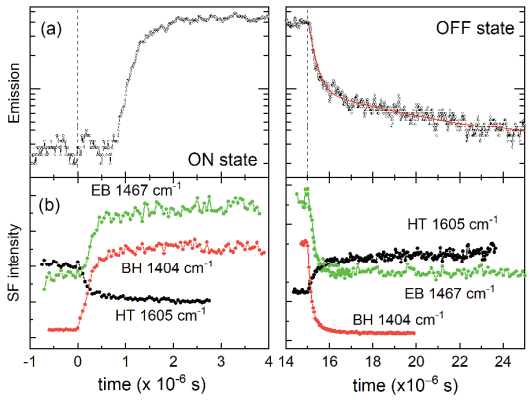

Fig. 6 (a) Transient EL emission from blue-OLED under application of the square wave pulse bias. (b) Corresponding time response of the SFG intensities of the peaks at 1404, 1467, and 1605 cm^{-1}.

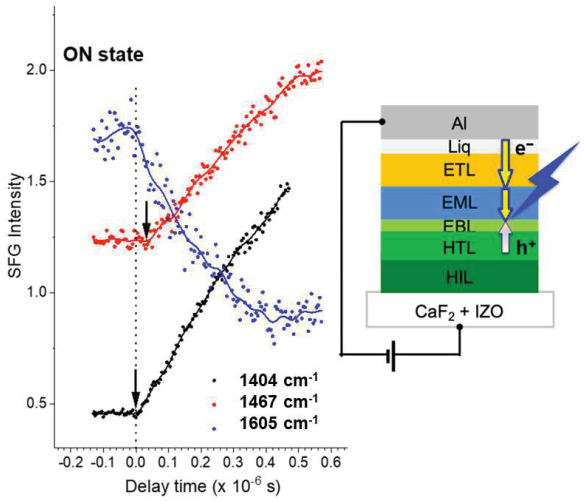

Fig. 7 Time-response of the SFG intensities at 1404, 1467, and 1605 cm^{-1}. Inset shows the Schematic illustration of the carrier behavior in the blue OLED.

of the SFG signal from the electron blocking material (red dots, 1467 cm^{-1}, EB01) shows about 30 ns delay from the rising edge of the BH01. This delay indicates the injected electrons are first accumulated at the electron transport layer side of the light emission layer interface, as sown in the inset of Fig. 7. Because part of the electrons can pass through the emission layer, the accumulated charges penetrate the emission layer. And then, it starts to re-accumulate at the interface between the emitting layer and the electron blocking layer, and recombines with holes, because holes cannot penetrate the emission layer.

For TTA process, the important thing is, the higher the charge density, the higher the efficiency of the TTA process. Therefore, we conclude that charge accumulation at electron blocking layer / emission layer interface forms a concentrated triplet region and induces TTA with high efficiency.

4 CONCLUSIONS

Electric-field induced doubly-resonant SFG spectroscopy has been developed and was applied to the intrinsic degradation analysis of OLEDs. Change of the molecular orientation due to the continuous driving stress was identified.

We also investigated the carrier behavior in a high-efficiency blue-OLED that employs the TTA phenomenon. We observed enhancements of the EFI-DR-SFG signals when we applied forward- or reverse-bias voltages to the blue OLEDs. The series of experimental EFI-DR-SFG measurements demonstrate that this technique is an effective non-destructive analytical tool for investigating the carrier behavior of the buried interfaces in multilayer organic devices with complicated operating mechanisms.

REFERENCES

[1] M. A. McCarthy, B. Liu, E. P. Donoghue, I. Kravchenko, D. Y. Kim, F. So, and A. G. Rinzler, “Low-Voltage, Low-Power, Organic Light-Emitting Transistors for Active Matrix Displays”, Science, Vol. 332, No. 6029, pp. 570–573 (2011).

[2] C. Adachi, “Third-generation organic electroluminescence materials”, Jpn. J. Appl. Phys. Vol. 53, No. 6, pp. 060101 (2014).

[3] C. W. Tang, and S. A. Vanslyke, “Organic electroluminescent diodes”, Appl. Phys. Lett. Vol. 51, pp. 913–915 (1987).

[4] T. Miyamae, N. Takada, and T. Tsutsui, “Probing buried organic layers in organic light-emitting diodes under operation by electric-field-induced doubly resonant sum frequency generation spectroscopy, Appl. Phys. Lett. Vol. 101, pp. 073304 (2012).

[5] T. Miyamae, N. Takada, T. Yoshioka, S. Miyaguchi, H. Ohata, and T. Tsutsui, “Rearrangement of the molecular orientation of Alq_3 in organic light-emitting diodes under constant current aging investigated using sum frequency generation spectroscopy”, Chem. Phys. Lett. Vol. 616–617, pp. 86–90 (2014).

[6] T. Miyamae, N. Takada, H. Ohata, and T. Tsutsui, “Direct probing of charge carrier behavior in multilayered organic light-emitting diode devices by time-resolved electric-field-induced sum-frequency generation spectroscopy”, Appl. Phys. Express, Vol. 10, pp. 102101 (2017).

[7] T. Miyamae, E. Ito, Y. Noguchi, and H. Ishii, “Characterization of the interactions between Alq_3 thin films and Al probed by two-color sum-frequency generation spectroscopy”, J. Phys. Chem. C, Vol. 115 pp. 9551–9560 (2011).

[8] E. Ito, Y. Washizu, N. Hayashi, H. Ishii, N. Matsuie, K. Tsuboi, Y. Ouchi, Y. Harima, K. Yamashita, and K. Seki, T. Miyamae, N. Takada, T. Tsutsui, “Spontaneous buildup of giant surface potential by vacuum deposition of Alq_3 and its removal by visible light irradiation”, J. Appl. Phys., Vol. 92, No. 12, pp. 7306–7310 (2002).

[9] T. Sato, T. Miyamae, H.Ohata, and T. Tsutsui, “Direct Observations of the Charge Behavior of a High-Efficiency Blue Organic Light-Emitting Diode under Operating Conditions using Electric-Field-Induced Doubly Resonant Sum-Frequency-Generation Vibrational Spectroscopy”, Org. Electron., Vol. 74, pp. 118–125 (2019).

[10] T. Suzuki, Y. Nonaka, T. Watabe, H. Nakashima, S. Seo, S. Shitagaki, S. Yamazaki, “Highly efficient long-life blue fluorescent organic light-emitting diode exhibiting triplet-triplet annihilation effects enhanced by a novel hole-transporting material”, Jpn. J. Appl. Phys., Vol. 53, pp. 052102 (2014).